Am J Cancer Res 2015;5(10):2998-3014
www.ajcr.us /ISSN:2156-6976/ajcr0009986

Original Article

Expression of DDX27 contributes to colony-forming ability of gastric cancer cells and correlates with poor prognosis in gastric cancer

Yoshiyuki Tsukamoto[1], Shoichi Fumoto[1,2], Tsuyoshi Noguchi[3], Kazuyoshi Yanagihara[4], Yuka Hirashita[1,5], Chisato Nakada[1], Naoki Hijiya[1], Tomohisa Uchida[1], Keiko Matsuura[1], Ryoji Hamanaka[6], Kazunari Murakami[5], Masao Seto[7], Masafumi Inomata[2], Masatsugu Moriyama[1]

Departments of [1]Molecular Pathology, [2]Gastroenterological and Pediatric Surgery, [5]Gastroenterology, [6]Cell Biology, Faculty of Medicine, Oita University, Oita, Japan; [3]Center for Community Medicine, Division of Surgery, Faculty of Medicine, Oita University, Oita, Japan; [4]Division of Pathology, Exploratory Oncology Research & Clinical Trial Center, National Cancer Center, Chiba, Japan; [7]Department of Pathology, Kurume University School of Medicine, Fukuoka, Japan

Received May 7, 2015; Accepted August 28, 2015; Epub September 15, 2015; Published October 1, 2015

Abstract: Previously, we have reported that gain at chromosome 20q13 is the most common genomic copy number aberration in gastric cancer (GC) (29/30 cases), and that among the genes located in this region, we have identified DDX27, whose expression level shows the highest correlation with genomic copy number, as a candidate therapeutic target for GC. Here, we analyzed the clinicopathological significance of DDX27 using immunohistochemistry and studied its functions using knockdown assays. We found that DDX27 was frequently upregulated in GC tissues (98 of 140 cases, 70%), and significantly associated with venous invasion and liver metastasis. Furthermore, multivariate analysis of GC patients showed that high expression of DDX27 was independently associated with poorer prognosis. In functional assays, knockdown of DDX27 reduced the ability of GC cells to form colonies both on conventional plates and soft agar, but had little effect on their invasiveness. We also found that knockdown of DDX27 reduced the viability of GC cells through inhibition of cell cycle progression independently of apoptosis. Interestingly, DDX27 depletion induced accumulation of TP53 in a TP53 wild-type cell line, AGS, but not in a TP53-deleted cell line, 44As3, although DDX27 knockdown commonly reduced the viability of both, indicating the TP53-dependent and independent cell cycle control of DDX27. Thus, our results suggest that expression of DDX27 contributes to colony formation by GC cells through cell cycle control and may be a potential therapeutic target for GC patients with chromosome gain at 20q13.

Keywords: Gastric cancer, RNA helicase, 20q13, DDX27, colony formation

Introduction

Although the clinical outcome of gastric cancer (GC) has gradually improved, the prognosis of patients with advanced disease is still disappointing. To improve the survival of patients with advanced GC, identification of novel biomarkers and targets is required for clinical management.

Previously, we and others have reported that chromosomal gain at 20q13 is the most common genomic copy number aberration in GC (50% to 97% of cases) [1-8]. Gain at 20q13 has also been observed at a high rate in many other types of solid tumors, including cancers of the colon, esophagus, breast, cervix, ovary, pancreas, prostate and bladder [9-16]. While some reports have shown that gain at 20q13 is frequent even in the initial phase of carcinogenesis [13, 17, 18], others have demonstrated a significant association of this aberration with poor survival in patients with colon and esophageal cancer [19, 20], progression of colon, ovarian, cervical and gastric cancers [9, 21-23], and liver metastasis of colon and esophageal cancers [24-26]. Thus, gain at 20q13 seems to affect various aspects of carcinogenesis, impli-

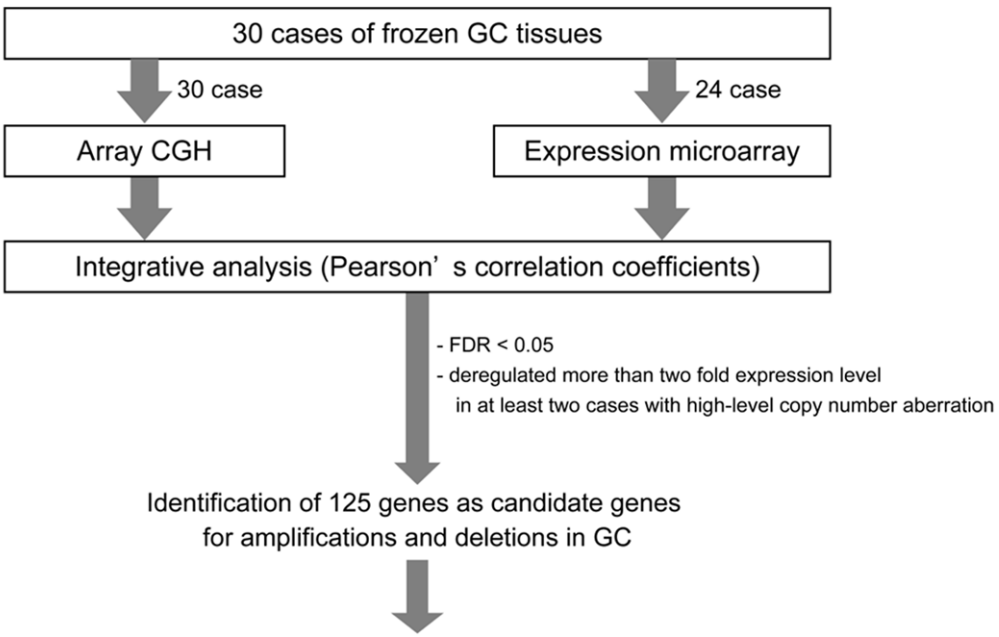

Probe name	Gene name	Description	Pearson's r	FDR	Fold change
A_23_P40194	**DDX27**	**DEAD (Asp-Glu-Ala-Asp) box polypeptide 27**	**0.71**	**0.00012**	**2.4**
A_24_P5935	KUA-UEV	ubiquitin-conjugating enzyme E2 variant 1	0.69	0.00019	1.7
A_23_P68472	DPM1	dolichyl-phosphate mannosyltransferase polypeptide 1, catalytic subunit	0.67	0.00033	1.5
A_23_P254179	ADNP	activity-dependent neuroprotector	0.66	0.00037	1.3
A_32_P205637	PARD6B	par-6 partitioning defective 6 homolog beta	0.62	0.00090	1.1
A_23_P338890	PTPN1	protein tyrosine phosphatase, non-receptor type 1	0.59	0.00190	1.3
A_24_P161463	C20orf199	chromosome 20 open reading frame 199	0.57	0.00281	2.1
A_23_P5995	ARFGEF2	ADP-ribosylation factor guanine nucleotide-exchange factor 2	0.54	0.00459	1.4

Figure 1. Identification of candidate target genes for amplifications and deletions in gastric cancer in our previous study. In our previous study, we analyzed 30 cases of GC for their genomic copy number aberrations and 24 cases for their gene expression profiles, and integrated the two data sets using a CGH-plotter [1]. To identify genes whose expression was upregulated along with an increase in copy number, Pearson's correlation coefficients between the copy number and expression level for each gene were calculated and significance was determined in terms of the false discovery rate (FDR), for which a multiple-comparison free statistical test based on 10000 random label permutations was performed. We identified 14 and 5 regions of amplifications and deletions in GC, respectively, and the 125 genes located in these regions were considered candidate targets for GC. Because amplification of 20q13 was detected in almost all cases (29/30, 97%), we focused on the genes in this region. Of the 8 genes identified as candidates for 20q13, DDX27 showed the highest correlation coefficient.

cating multiple targets on this region rather than a sole target, in contrast to other well characterized amplifications that involve a sole target, such as MYC at 8q24, EGFR at 7p12 and ERBB2 at 17q21. Therefore, identification of targets for 20q13 gain may help to shed further light on gastric carcinogenesis and assist the establishment of effective therapeutic strategies.

It has been reported that several genes are upregulated along with a copy number increase at 20q13, and play specific and important roles in carcinogenesis, such as AURKA and TPX2 in mitotic spindle organization [27], ZNF217 in transcriptional regulation of differentiation-related genes [28] and ADRM1 in deubiquitination as a 19S proteasomal cap-associated protein [29]. In our previous study, we identified DDX27 as a candidate target for amplification at 20q13, since its expression showed the highest correlation with the genomic copy number among the genes located on the minimum common region of the 20q13 amplicon [1] (**Figure 1**). DDX27 is a member of the DEAD/DExH box family of RNA helicases, which have been shown to play various roles in RNA biogenesis including translation, ribosome biogenesis, pre-mRNA splicing and nucleo-cytoplasmic RNA transport [30]. In addition to the roles of

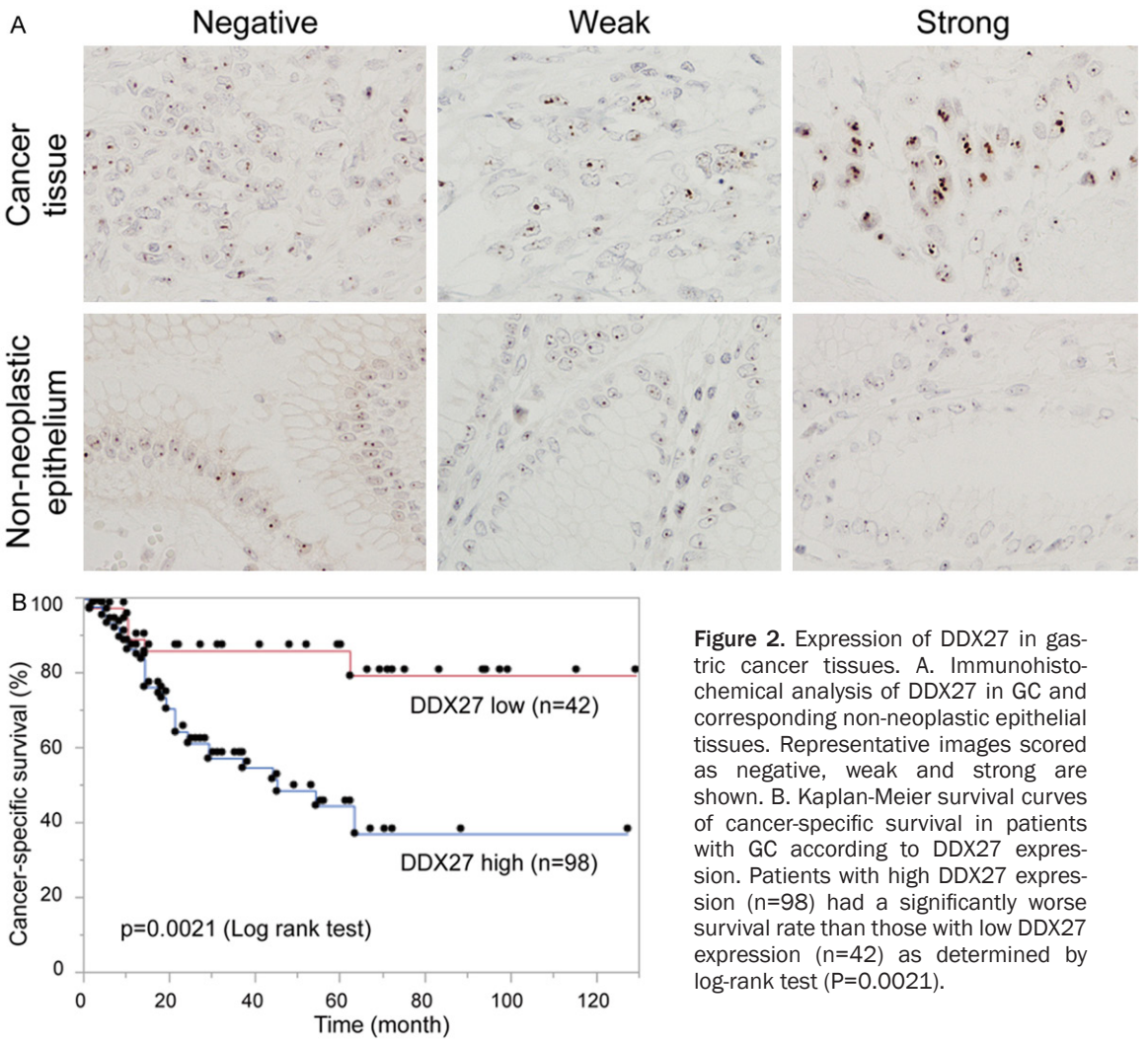

Figure 2. Expression of DDX27 in gastric cancer tissues. A. Immunohistochemical analysis of DDX27 in GC and corresponding non-neoplastic epithelial tissues. Representative images scored as negative, weak and strong are shown. B. Kaplan-Meier survival curves of cancer-specific survival in patients with GC according to DDX27 expression. Patients with high DDX27 expression (n=98) had a significantly worse survival rate than those with low DDX27 expression (n=42) as determined by log-rank test (P=0.0021).

this family in RNA biogenesis, recent studies have also suggested their involvement in carcinogenesis. For example, DHX29 has been reported to be upregulated in glioblastoma, melanoma and ovarian cancer, and to promote proliferation of cancer cells [31]. Whereas DDX5 is reportedly required for proliferation of breast cancer cells [32]. Furthermore, Fukawa et al. have reported that DDX31 is an independent prognostic factor in patients with renal cell carcinoma, contributing to the growth of renal cancer cells [33]. To date, however, details of the functions and dysregulation of DDX27 in malignant tumors have remained largely unclear, except for one report [34].

In the present study, to determine the significance of DDX27 upregulation in GC cells, we performed immunohistochemical analysis using tissue sections from 140 GC patients and knockdown assays using GC cell lines.

Materials and methods

Patients and tissue samples

A total of 140 tumor tissue samples were obtained from GC patients who underwent gastric resection at Oita University Hospital. None of the patients received preoperative chemotherapy. Written informed consent was obtained from all of the patients, and the study was approved by Oita University ethics committee. Cancer-specific survival (CSS) was calculated from the date of surgery to the date of cancer-related death or last day of follow-up. GCs were classified according to the criteria of the Japanese Classification of Gastric Cancer [35], except for histological type, which was classified according to the Lauren classification [36]. The median follow-up period for patient survival was 21 months (range, 1-129 months). For analysis of the association between liver or

Table 1. Sequences of primers and targets for siRNA and shRNA

Genes	Sequence	Method
DDX27	5'-AGATTGAGAAAGTTCGAAA-3'	siDDX27
DDX27	5'-AGGTGCACTCTGTCACCAG-3'	DDX27sh2
DDX27	5'-AGGAAGACCTTCAAGAGAA-3'	DDX27sh3
45S pre-rRNA	5'-CCATAACGGAGGCAGAGACA-3'	Reverse transcription
45S pre-rRNA	5'-GCCTTCTCTAGCGATCTGAGAG-3'	RT-PCR (Forward)
45S pre-rRNA	5'-CCATAACGGAGGCAGAGACA-3'	RT-PCR (Reverse)
47S pre-rRNA	5'-CGACGTCACCACATCGATCG-3'	Reverse transcription
47S pre-rRNA	5'-GCTGACACGCTGTCCTCTGG-3'	RT-PCR (Forward)
47S pre-rRNA	5'-GAGAACGCCTGACACGCACG	RT-PCR (Reverse)

peritoneal metastasis and DDX27 expression, we enrolled patients for whom 5 years of follow-up data for liver or peritoneal metastasis were available.

Immunohistochemistry

Immunohistochemistry was performed as described previously [1] with slight modifications, in that sections were immersed in Antigen Retrieval buffer, pH 9.0 (Nichirei, Tokyo, Japan), and autoclaved at 120°C for 10 min for antigen retrieval. Anti-DDX27 antibody (1:100, sc-81074; Santa Cruz Biotechnology, Santa Cruz, CA, USA) was used as the primary antibody. The intensity of nucleolar DDX27 immunoreactivity in tumor cells was compared with that in adjacent non-neoplastic epithelium and classified as negative (as intense as that in adjacent non-neoplastic epithelium), weak (slightly more intense than that in adjacent non-neoplastic epithelium) or strong (obviously more intense than that in adjacent non-neoplastic epithelium) (**Figure 2A**). If more than 10% of tumor cells were strongly stained, the patients were considered to have high expression of DDX27.

Array CGH and data analysis

Array-CGH analysis was performed using high-resolution 244K 60-mer oligonucleotide CGH arrays, as described previously (Agilent Technologies, Palo Alto, CA, USA) [23]. Two micrograms of DNA extracted from GC cell lines and an equal amount of control DNA, which was a mixture of genomic DNA extracted from peripheral blood cells of eight healthy male volunteers, were subjected to array-CGH. Microarray images were analyzed as described previously using Feature Extraction v.9.5.3.1 (Agilent Technologies) and the DNA Analytics v.4.0 software (Agilent Technologies) [23]. Following normalization, the log2ratio of Cy5 (tumor) to Cy3 (Control) was calculated. Genomic copy number gains and losses were determined by the ADM-2 algorithm at a threshold of 8. To detect genomic aberrations, we set the following aberration filter parameters: minimum number of probes in region, 4; minimum absolute average log2ratio for region, 0.585; maximum number of aberrant regions, 100000; percentage penetrance per feature, 0. We set the minimum absolute average log2ratio at 0.585 to detect regions showing a change in the averaged copy number equal to or more than 1.5-fold (log2 (1.5)=0.584963). The data obtained in the array CGH analysis are available at GEO (www.ncbi.nlm.nih.gov/geo/), under Accession No. GSE67604.

Cell culture and siRNA transfection

IM95, NUGC4, OSUM1, FU97, MKN74 and MKN1 were obtained from the JCRB in 2007. SNU638 and SNU484 were obtained from the Korean Cell Line Bank in 2010. AGS was obtained from the American Type Culture Collection in 2010. 44As3 and SH101P4 were established and reported previously [37, 38]. All cells were cultured under the recommended conditions. ON-TARGET plus human DDX27 (siDDX27) (#1 of 4 individual siRNAs in SMART pool siRNA targeting DDX27, **Table 1**) and non-targeting pooled (siCont) siRNAs were purchased from Dharmacon (GE Dharmacon, Lafayette, CO, USA) and used for transfection at a concentration of 5 nM using RNAiMAX (Invitrogen/Life Technologies, Carlsbad, CA, USA).

Construction of lentivirus vectors and establishment of stable cell lines

For rescue experiments, we generated a siRNA-resistant mutant of DDX27 cDNA, designated as DDX27r, by introducing a silent mutation in the coding region of wild-type DDX27 cDNA, which was obtained from Origene (OriGene, Rockville, MD, USA), by using a QuickChange Lightning Site-Directed Mutagenesis Kit (Agilent Technologies) (366-372; GAAAGTT to AAAGGTC). DDX27r was amplified by PCR, subcloned into pENTR/D-TOPO, and then recom-

Table 2. Associations between clinicopathological features and DDX27 expression

		DDX27 staining		
Features	Cases	Low	High	*P*-value[a]
Gender				0.5452
Female	41	14	27	
Male	99	28	71	
Age				0.0737
≤65	46	18	26	
>65	96	24	72	
Histological type[b]				0.3572
Intestinal	74	25	49	
Diffuse	66	17	49	
T-stage				0.5583
T1, T2	47	16	31	
T3, T4	93	26	67	
N-stage				0.2964
Negative	37	14	23	
Positive	102	28	74	
TNM stage				0.2733
I/II	73	25	48	
III/IV	67	17	50	
Lymphatic Invasion				1.000
Negative	29	9	20	
Positive	111	33	78	
Venous Invasion				0.002
Negative	78	32	46	
Positive	62	10	52	
Peritoneal metastasis[c]				0.0943
Negative	55	19	36	
Positive	22	3	19	
Not analyzed	63			
Liver metastasis[c]				0.016
Negative	59	21	38	
Positive	18	1	17	
Not analyzed	63			

[a]Fisher's exact test. [b]Tumors were classified according to the Lauren classification. [c]We analyzed 77 patients whoes 5 year follow-up data about metastasis status were obtained.

bined into pLenti6.3/V5-DEST by Gateway LR clonase (Invitrogen). For shRNA-mediated knockdown experiments, we purchased a pGIPZ vector set carrying shRNAs against DDX27 (Open Biosystems/GE Dharmacon). Among the set of 5 shRNA vectors, shRNA#2 and #3 (**Table 1**) were digested at the MluI and XhoI sites and the resulting shRNA fragments were subcloned into the pTRIPZ inducible lentiviral vector (Open Biosystems). Lentiviruses carrying pLenti6.3/V5-DEST and pTRIPZ constructs were packaged with 293T cells using the ViraPower Lentiviral Expression System (Invitrogen) and TransLenti Viral Packaging System (GE Healthcare), respectively. We infected 44As3 and MKN74 cells with lentiviruses carrying pLenti6.3/V5-DEST empty (44/Emp), DDX27r (44/DDX27r) or pTRIPZ shRNA#2 (44/DDX-27sh2), and pTRIPZ shRNA#3 (74/DDX27sh3), respectively, in accordance with the manufacturers' instructions. After selection with 4 μg/ml blasticidin and 0.4 μg/ml puromycin for the pLenti6.3/V5-DEST and pTRIPZ constructs, respectively, they were cloned by the limited dilution method.

Western blotting

Western blotting was performed as described previously [39]. The primary antibodies used were: anti-DDX27 (1:500, Atlas Antibodies, Stockholm, Sweden), anti-tubulin (1:4000, Cell Signaling Technology, Danvers, MA, USA), anti-p53 (1:15, Dako, Glostrup, Denmark) and anti-p21 (1:500, Cell Signaling Technology).

Invasion assay

Invasiveness of 44As3 cells was measured using FluoroBlock Cell Culture Inserts (Corning, Corning, NY, USA). The filters, with an 8-μm pore size, were precoated with 1 μg/40 μl/filter of fibronectin on their lower surfaces and dried at room temperature overnight, and then coated with matrigel on their upper surfaces at a concentration of 5 μg/20 μl/filter and dried. The filters were washed and dried just before use. 44As3 cells (1×10^5) transfected with siRNAs for 48 h were added to the upper compartment of the chamber and incubated in 10% FBS-RPMI for 16 h. Invaded cells were incubated with Calcein-AM solution (Dojindo, Kumamoto, Japan) and quantified by Infinite M200 PRO (TECAN, Maennedorf, Switzerland).

Cell proliferation, colony formation and apoptosis assay

For the cell proliferation assay, we transfected siRNAs into AGS, 44As3 and MKN74 cells for 72 or 96 h, and measured the viabilities of the cells using the CellTiter96 aqueous one solution cell proliferation assay (Promega, Madison, WI, USA). For colony formation assay, 500 cells transfected with siRNA for 48 h were plated in 10-cm dishes and cultured for 14 to 24 days. The resulting colonies were fixed with 10% buffered formalin, stained with 0.05% toluidine

Table 3. Univariate and multivariate analyses of prognostic features in GC

Features	Univariate[a]	Multivariate[b]		
	P-value	Hazard ratio	95% Confidence interval	*P*-value
Age				
≤65/ >65	**0.0454**	1.69	0.81-3.91	0.1683
Sex				
Female/Male	0.0585	-	-	-
Histological type				
Intestinal/Diffuse	0.9835	-	-	-
Lymphatic invasion				
Negative/Positive	**0.0128**	1.32	1.32-0.39	0.6774
Venous invasion				
Negative/Positive	**0.0001**	1.15	0.55-2.52	0.722
Tumor depth				
T1, T2/T3, T4	**<0.0001**	4.05	1.44-14.56	**0.0065**
Lymph node metastasis				
Negative/Positive	**0.0044**	1.38	0.54-4.28	0.523
DDX27 expression				
Low/High	**0.0021**	2.33	1.01-6.39	**0.0465**

Values in bold indicate below 0.05. a, Log-rank test. b, Cox proportional hazards model.

blue solution (pH 7.0) (Wako, Osaka, Japan) and quantified using Image J 1.48v (National Institutes of Health, USA). For the apoptosis assay, we transfected siRNA into AGS and 44As3 cells for 72 h and measured the cytoplasmic oligonucleosomal fragments using a Cell Death Detection ELISA PLUS kit (Roche, Basel, Switzerland).

Soft agar colony formation assay

After treatment with or without 1 μg/ml doxycyclin (Dox) for 48 h, 44/DDX27sh2 and 74/DDX27sh3 cells (4.5×103/well in 96-well plates) were cultured in a cell agar layer containing 10% FBS-RPMI and 0.4% agar (Sigma) on a base agar layer containing 10% FBS-RPMI and 0.6% agar under conditions with or without 1 μg/ml Dox. 44As3 and MKN74 were grown for 8 and 11 days, respectively, and their colonies were observed using a light microscope. To quantify the efficiency of colony formation, the CytoSelect 96-Well Cell Transformation Assay (Cell Biolabs, San Diego, CA, USA) was used.

Tumorigenicity assay

44/DDX27sh2 cells were harvested and resuspended in OPTI-MEM (Life Technologies) at a concentration of 2.5×10^7 cells/ml. A total of 5×10^6 cells were injected subcutaneously into the left flank of 8week-old male BALB/c nude mice. The mice were either left untreated or administered Dox using a combination of oral gavage (10 mg/100 μl in sterilized water) once every three days and addition to drinking water (0.6 mg/ml in 5% sucrose) for 36 days. The treatment was started the day before the injection. Tumor volume was calculated at 2, 3 and 5 weeks after the injection using the formula: (width × length × height)/2. All protocols for animal studies were approved by the animal ethics committee at Oita University (Approval No K008001).

Cell cycle analysis

Cells transfected with siRNA for 96 h were fixed with 70% ethanol and stained with propidium iodide staining buffer (5 mg/ml DNase-free RNase A and 50 μg/ml propidium iodide in PBS) for 20 min. The DNA content of the cells, which reflects the cell cycle distribution, was determined using a FACScalibur flow cytometer (BD, Franklin Lakes, NJ, USA). The rate of DNA synthesis was determined 72 h after transfection with siRNAs using a Cell Proliferation ELISA BrdU kit (Roche).

Immunocytochemistry

Immunocytochemistry was performed as described previously [40]. The primary antibodies used were: anti-phospho-histone H3 (pHH3) (Cell Signaling Technology), anti-DDX27 (Atlas Antibodies) and anti-FBL (Santa Cruz).

Quantitative RT-PCR

To estimate the rate of ribosomal RNA transcription, we performed quantitative RT-PCR to measure 45S and 47S pre-ribosomal RNA (pre-rRNA) using LightCycler 480 SYBR Green I Master Mix (Roche) in accordance with previous studies [33, 41]. The primer sequences used for cDNA synthesis and amplification for pre-rRNAs are detailed in **Table 1**.

Measurement of global translation rate

Cells transfected with siRNAs for 72 h were incubated with methionine-free RPMI for 10 min, and then labeled with 2 MBq/ml of [^{35}S]

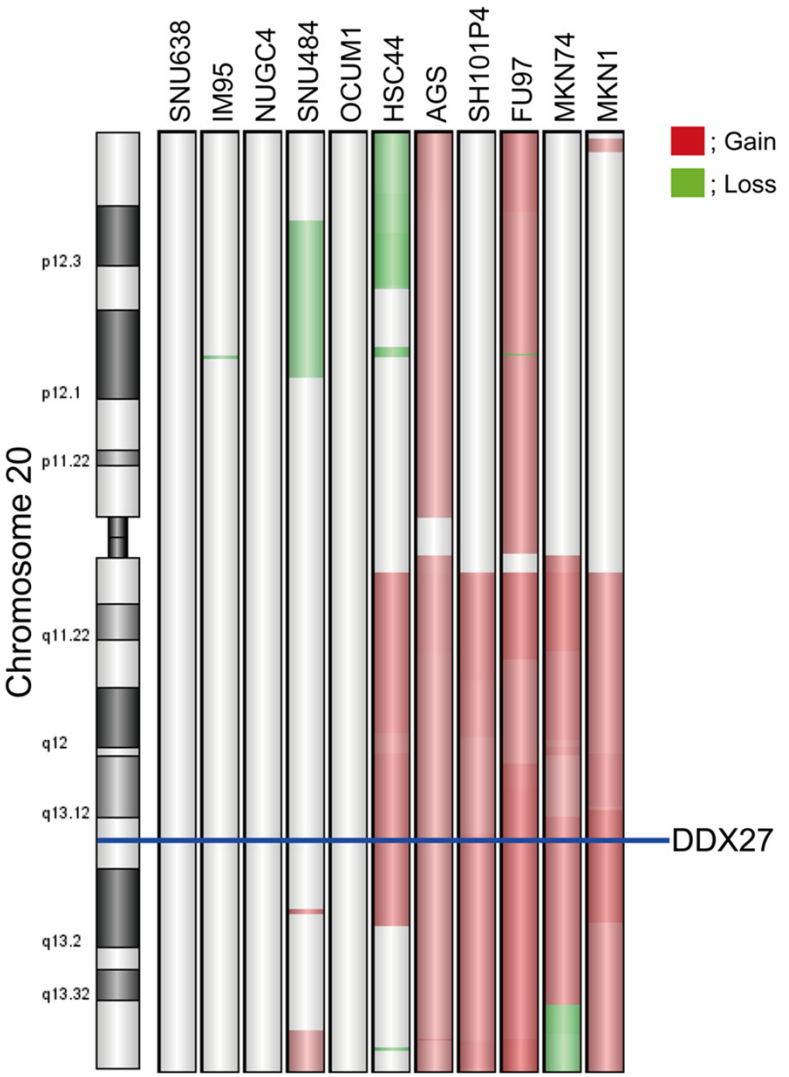

Figure 3. Status of 20q copy number in GC cell lines. The genomic copy number status of chromosome 20 in 11 GC cells was analyzed by using array CGH. Genomic regions of copy number gain and loss are indicated by red and green, respectively. Location of *DDX27* is indicated by a blue line. Expression of DDX27 protein in these cell lines is shown in **Figure 4A**, except for HSC44, which was the parental cell line of 44As3 [38].

methionine (PerkinElmer Japan, Tokyo, Japan) for 30 min. After washing with PBS, the cells were lysed on ice for 20 min in 0.1% SDS-modified RIPA buffer [39], then centrifuged at 15,000 rpm at 4°C for 20 min. The resulting lysates (50 μg samples) were resuspended in Laemmli sample buffer and subjected to SDS-PAGE using 10% gel. Radio-labeled proteins were visualized using a Typhoon FLA7000 (GE Healthcare).

Statistical analysis

The association between DDX27 expression and clinicopathological factors was determined by Fishers's exact test. Kaplan-Meier curves were drawn and differences between the curves were calculated by the log-rank test, using JMP 11.0 (SAS Institute, Cary, NC, USA). Univariate analysis was performed using the Kaplan-Meier method, and significance was determined by log-rank test. Factors shown to be of prognostic significance in the univariate analyses were evaluated in a multivariate Cox regression model using the likelihood ratio test of the stratified Cox proportional hazards model by JMP. Differences in invasion, colony formation, proliferation, apoptosis, cell cycle and qRT-PCR assays were analyzed by two-sided Student's t test by StatView (SAS Institute). Data are reported as mean values ± SD of triplicate or quadruplicate determinations. Differences were considered statistically significant at $P<0.05$.

Results

Expression of DDX27 in gastric cancer tissues

To investigate the clinicopathological significance of DDX27 expression in gastric cancer, immunohistochemistry was performed in 140 cases of GC. Immunoreactivity for DDX27 was observed in the nucleolus of both non-neoplastic epithelium and cancer cells (**Figure 2A**). Only faint immunoreactivity was observed in most of the non-neoplastic epithelial cells. DDX27 staining was observed in many GC tissues, although the proportion and intensity of the immunoreactivity varied across individuals (**Figure 2A**). The intensity of nucleolar DDX27 staining in GC cells was classified as negative, weak or strong (**Figure 2A**). Cases in which more than 10% of cancer cells exhibited strong staining were considered to have high expression of DDX27. Of the 140 cases, 98 (70%)

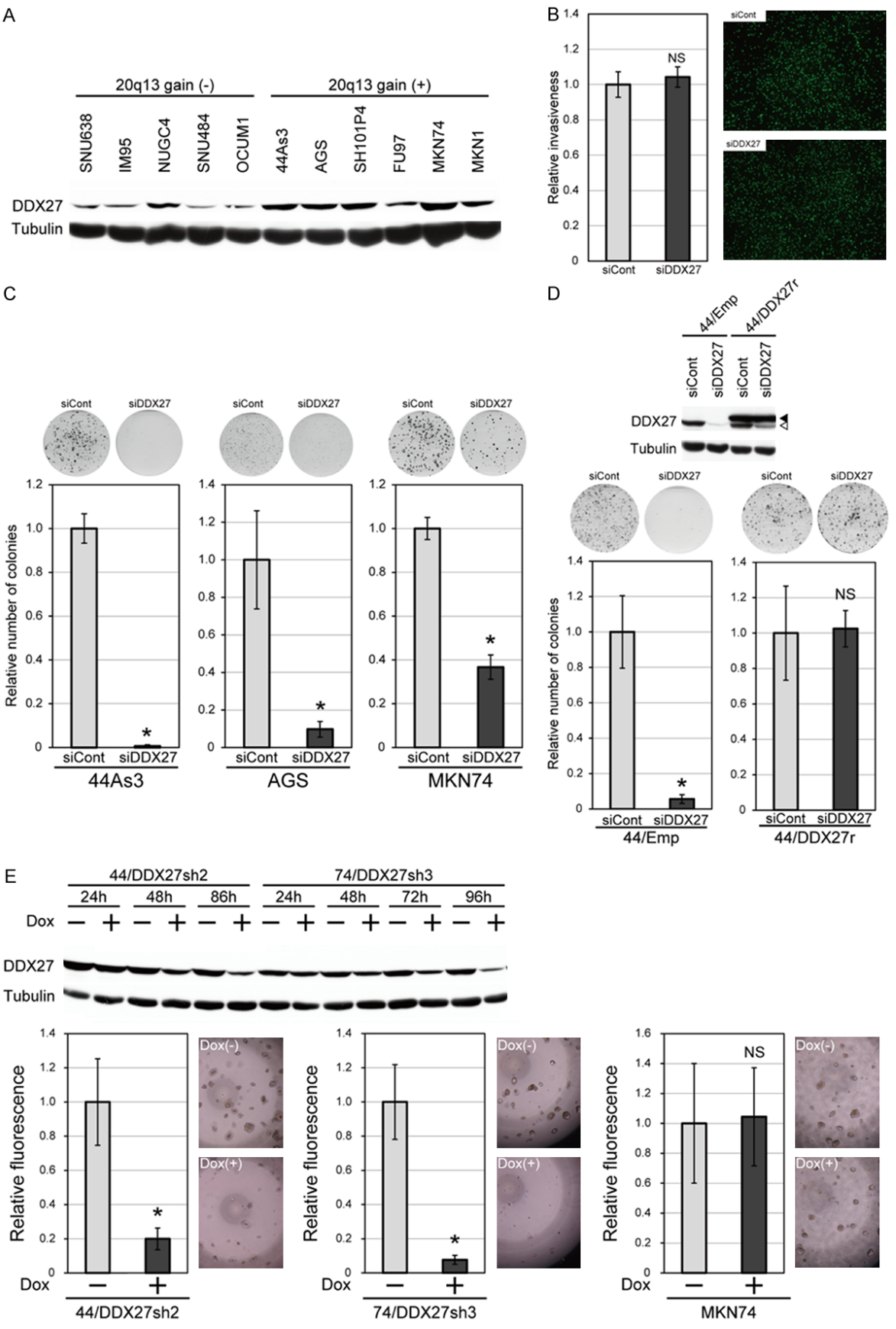
A
20q13 gain (-)
20q13 gain (+)
SNU638
IM95
NUGC4
SNU484
OCUM1
44As3
AGS
SH101P4
FU97
MKN74
MKN1
DDX27
Tubulin
B
Relative invasiveness
NS
siCont
siDDX27
C
Relative number of colonies
siCont
siDDX27
44As3
AGS
MKN74
D
44/Emp
44/DDX27r
DDX27
Tubulin
Relative number of colonies
NS
44/Emp
44/DDX27r
E
44/DDX27sh2
74/DDX27sh3
24h
48h
86h
72h
96h
Dox
DDX27
Tubulin
Relative fluorescence
Dox(-)
Dox(+)
44/DDX27sh2
74/DDX27sh3
NS
MKN74

Figure 4. DDX27 contributes to the colony-forming ability of GC cells but not to their invasiveness. A. Western blot analysis of DDX27 expression in GC cell lines. Status of copy number gain at 20q13 was determined by array CGH analysis (**Figure 3**). Tubulin was used as an internal control. B. Invasiveness of 44As3 cells transfected with siCont or siDDX27 was determined by matrigel invasion assay (n=3). Representative fluorescence images of invaded cells are shown. The fluorescence intensity of siCont cells was set at 1. C. Effect of DDX27 knockdown on colony formation by 44As3, AGS and MKN74 cells (n=3). Representative images of the resulting colonies are shown above the graph. The number of colonies transfected with siCont was set at 1. D. 44/Emp and 44/DDX27r were transfected with siCont or siDDX27, and subjected to Western blotting (upper) and colony formation (lower) assays. In Western blots, bands indicated by filled and empty arrowheads represent V5-tagged and endogenous DDX27, respectively. E. For Western blotting, 44/DDX27sh2 and 74/DDX27sh3 were treated with 1 μg/ml doxycycline for the indicated periods before cell lysis. For soft agar colony formation assay, 44/DDX27sh2 and 74/DDX27sh3 were treated with 1 μg/ml doxycycline for 48 h before culture in soft agar containing 1 μg/ml Dox (n=3 or 4). The intensity of fluorescence in Dox-negative cells was set at 1. The negligible effect of Dox on colony formation by MKN74 ruled out the possibility of an unexpected effect of Dox in 44/DDX27sh2 and 74/DDX27sh3. *P<0.05. NS; not significant.

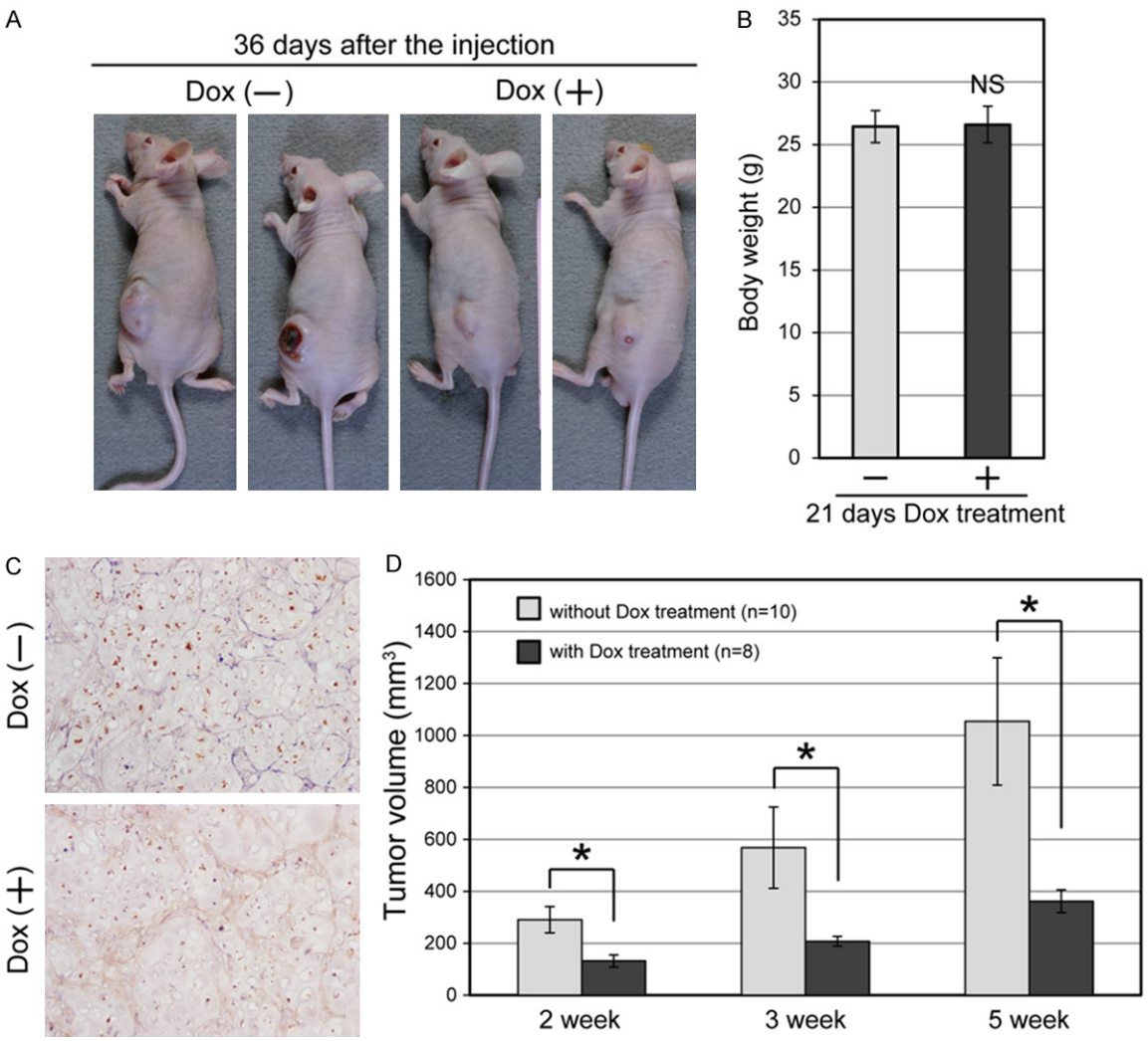

Figure 5. Knockdown of DDX27 inhibits in vivo tumorigenicity. A. 44/DDX27sh2 (5×106 cells) were subcutaneously injected into the left flank of nude mice and treated with or without Dox for 36 days as described in Materials and Methods. Two representative images of xenografts from each group are shown. B. Difference in weight gain of the groups with (n=8) or without (n=10) was determined by two-sided Student's t test. Dox treatment for 21 days did not cause weight loss. Data are reported as mean values ± SD. C. Suppression of DDX27 expression after the treatment of Dox for 36 days was confirmed by immunohistochemistry using anti-DDX27 antibody. Nucleolar expression of DDX27 was substantially suppressed in a Dox-treated xenograft. D. Differences in the tumor growth between dox-treated (n=8) and -untreated (n=10) groups at 2, 3 and 5 weeks after the injection were determined by two-sided Welch's t-test. Data are reported as mean values ± SE. *P<0.05.

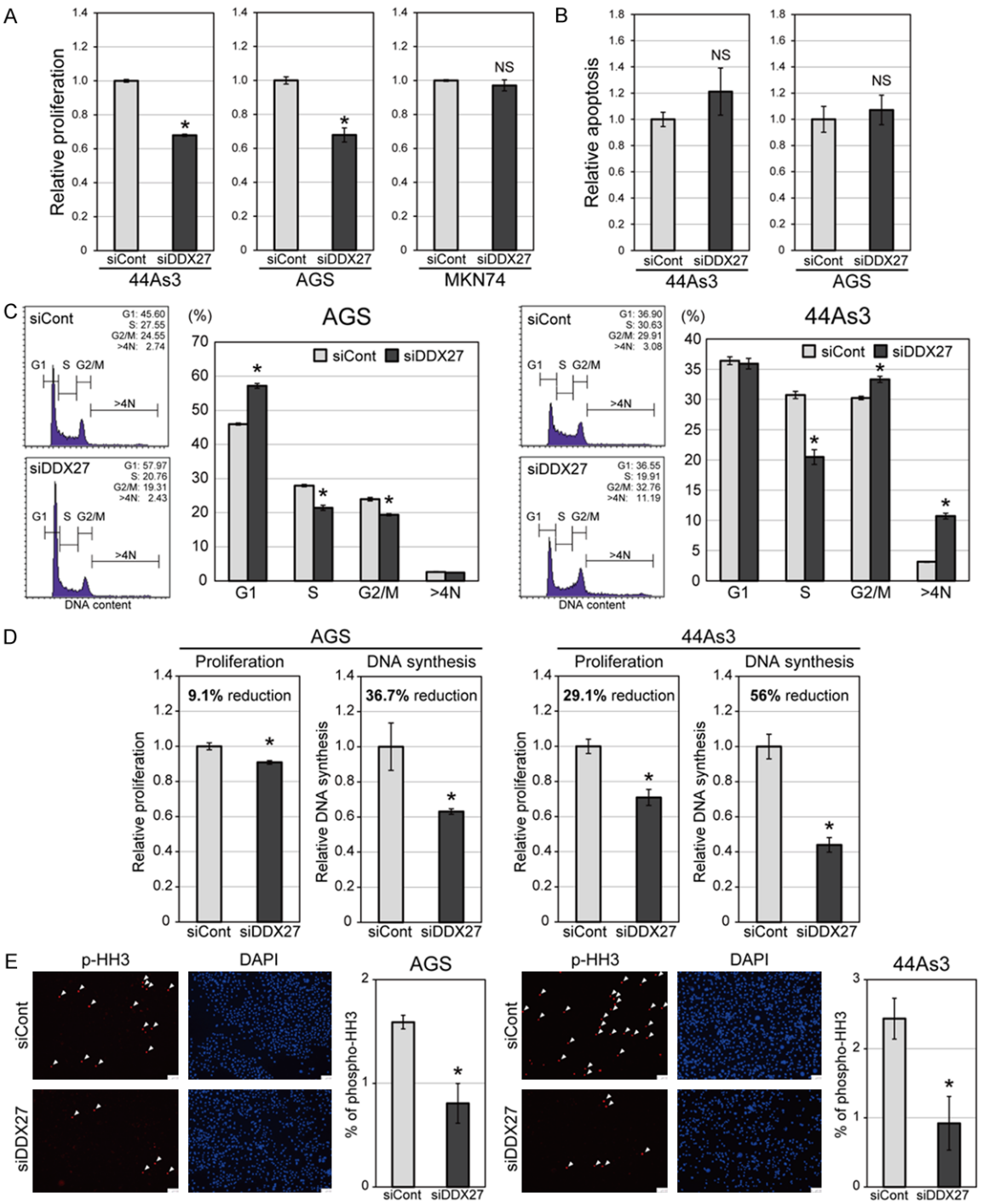

Figure 6. DDX27 contributes to colony-forming ability by regulation of cell cycle progression, but not apoptosis. A. Viabilities of 44As3, AGS and MKN74 cells were determined by MTS assay at 96 h after transfection with siCont or siDDX27 (n=4). The intensity of absorbance 492 nm for siCont was set at 1. B. Cytoplasmic oligonucleosomal fragment was measured for apoptosis at 72 h after transfection of 44As3 and AGS cells with siCont or siDDX27 (n=3 or 4). C. AGS and 44As3 cells were transfected with siCont or siDDX27 for 96 h and subjected to FACS analysis to determine the distribution of cells in the G1, S, and G2/M phases, and aneuploidy (DNA content greater than 4N) (n=3). Representative FACS profiles are shown on the left side of the graphs. D. AGS and 44As3 cells were transfected with siCont or siDDX27 for 72 h and subjected to proliferation and DNA synthesis assays (n=4). Percentage reductions in proliferation or DNA synthesis are shown in the graphs. E. AGS and 44As3 cells were transfected with siCont or siDDX27 for 96 h and subjected to immunocytochemistry using anti-p-HH3 antibody to label mitotic cells (n=3). Nuclei were counterstained by DAPI. Representative images are shown on the left side of the graphs. White

arrowheads indicate p-HH3-positive cells. The proportion of p-HH3-positive cells was calculated by dividing the number of cells positive for p-HH3 by the number of nuclei stained with DAPI, counted by Image J 1.48v in 4 separate fields for each sample. *P<0.05. NS; not significant.

showed high expression of DDX27 in cancer tissues. DDX27 staining was not associated with histological type, depth of invasion, lymph node metastasis or tumor stage, but was associated with the frequency of venous invasion (*P*=0.0016) and liver metastasis (*P*=0.0159) (**Table 2**). Kaplan-Meier survival analysis with the log-rank test showed that high DDX27 expression was significantly associated with poorer CSS (**Figure 2B**). Univariate analysis revealed that age, lymphatic invasion, venous invasion, tumor depth, lymph node metastasis and DDX27 expression were associated with CSS (*P*<0.05) (**Table 3**). Multivariate analysis revealed that DDX27 expression was an independent predictor of CSS (P=0.0465), as well as tumor depth (P=0.0065) (**Table 3**).

DDX27 contributes to colony formation by gastric cancer cells through regulation of the cell cycle independently of apoptosis

In order for cancer cells to undergo the full process of metastasis, enhanced abilities for invasion, survival and colony formation are required [42]. Since DDX27 expression in GC tissues was associated with liver metastasis (**Table 2**), we next addressed the involvement of DDX27 in invasiveness and colony formation by gastric cancer cells. As we expected from our previous study [1], cell lines showing 20q13 gain, such as 44As3, AGS and MKN74, tended to show a higher level of DDX27 expression than those without 20q gain (**Figures 3** and **4A**). Knockdown of DDX27 did not affect the invasiveness of 44As3 cells (**Figure 4B**), but drastically inhibited the colony-forming ability of 44As3, AGS and MKN74 cells (**Figure 4C**). Notably, stable expression of RNAi-resistant DDX27 (DDX27r) completely rescued colony formation ability after transfection with siDDX27 (**Figure 4D**), suggesting a specific effect of DDX27 siRNA in reducing the number of colonies formed. Knockdown of DDX27 also inhibited colony formation in soft agar (**Figure 4E**). Furthermore, we showed that knockdown of DDX27 inhibited tumorigenicity in vivo (**Figure 5**). Taken together, these results suggested that DDX27 contributes to colony formation by GC cells but has a less marked effect on their invasiveness. It was noteworthy that we were unable to observe enhancement of proliferation, colony formation and invasion of the DDX27 low-expressing GC cell line, SNU638, upon transient overexpression of DDX27 (**Figure 4A**, data not shown). A number of possible reasons could have accounted for this. Firstly, in addition to DDX27 overexpression, other gene alteration(s), such as overexpression, downregulation or mutation of other gene(s), might be required in order for GC cells to gain enhanced oncogenic abilities, a situation similar to co-occurrence of oncogenic ras and inactivation of TP53 [43], and co-expression of MYC and BCL2 [44]. Secondly, the growth and survival of GC cells with low DDX27 expression might depend on a pathway other than the DDX27-related pathway. Thirdly, the level of expression in a cell might be critical in order for DDX27 to exert its oncogenic functions, and transient overexpression of DDX27 may not work well in SNU638 cells. In fact, it has been reported that an optimal level of overexpression is required in order to achieve a gain-of-function phenotype for Nucleostemin, which functions as an oncogene in the nucleolus [45]. These issues will need to be investigated further by determining the mechanism whereby DDX27 contributes to colony formation by GC cells and the relationship between the level of DDX27 expression and its oncogenic activity. Currently, we are investigating these possibilities as an independent project in our laboratory.

To determine whether the suppression of colony formation by DDX27 knockdown is mediated through induction of apoptosis or/and inhibition of cell cycle progression, we performed cell death detection using ELISA and FACS analyses. Because proliferation of 44As3 and AGS cells was suppressed by DDX27 knockdown even in a short-term (96 h) proliferation assay (**Figure 6A**), we used these cell lines for apoptosis and cell cycle assays. Knockdown of DDX27 did not affect the amount of cytoplasmic oligonucleosomal fragment (**Figure 6B**), but caused significantly different patterns of cell cycle distribution in the two cell lines (**Figure 6C**). After transfection with DDX27 siRNA, AGS cells showed an increased proportion of cells in G1 phase and a decreased proportion in S and G2/M phase (**Figure 6C**, left), whereas 44As3

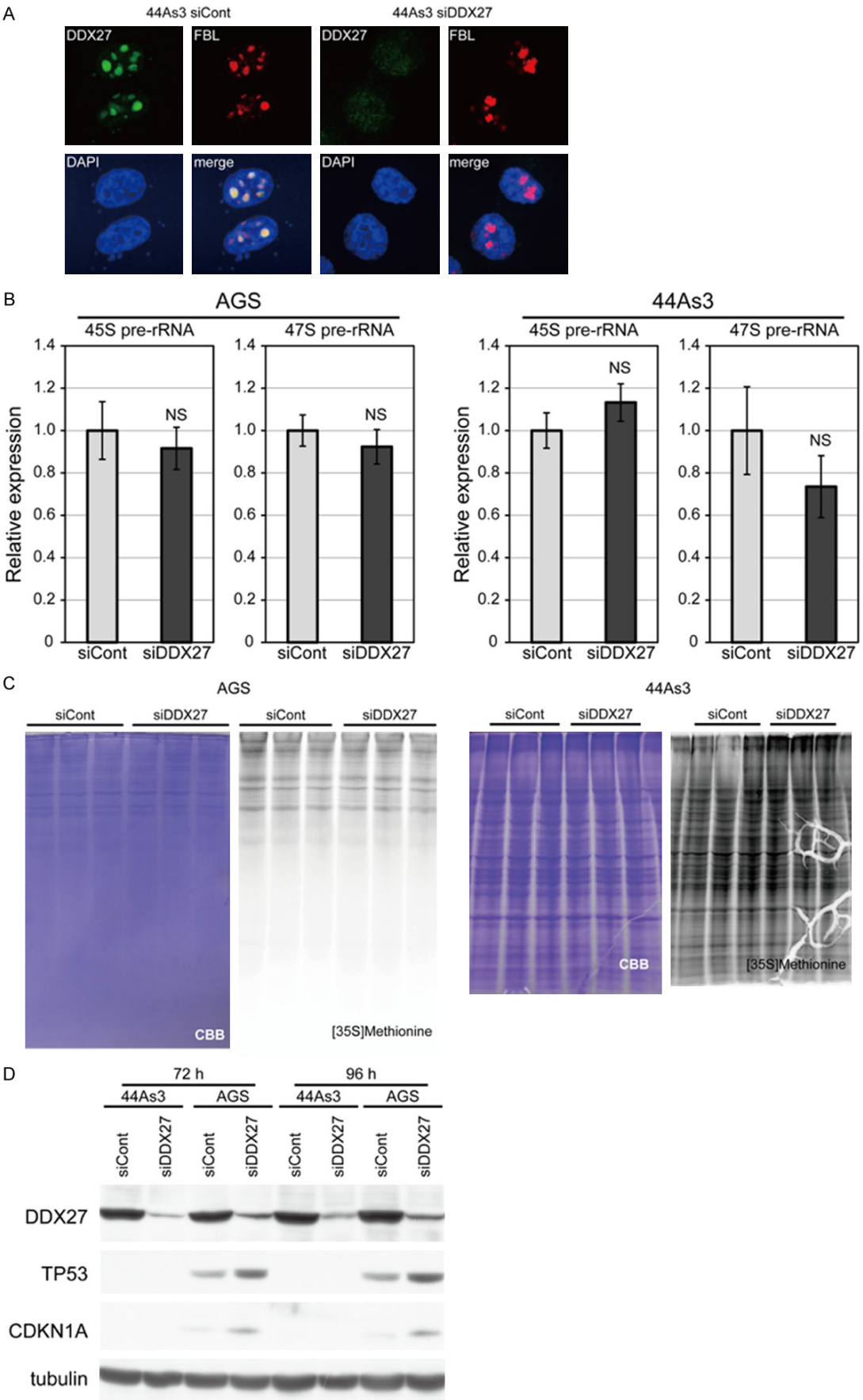
A
44As3 siCont
44As3 siDDX27
DDX27
FBL
DAPI
merge
B
AGS
44As3
45S pre-rRNA
47S pre-rRNA
Relative expression
NS
siCont
siDDX27
C
AGS
44As3
siCont
siDDX27
CBB
[35S]Methionine
D
72 h
96 h
44As3
AGS
DDX27
TP53
CDKN1A
tubulin

Figure 7. Knockdown of DDX27 has little effect on global protein synthesis, but induces TP53 in TP53 wild-type cells. A. Immunocytochemistry revealed that DDX27 co-localizes with FBL, a marker of the nucleolus, in 44As3 cells transfected with siCont. Knockdown of DDX27 completely diminished the nucleolar immunoreactivity for DDX27, suggesting the specific detection of nucleolar DDX27 by this antibody. B. To determine the rate of pre-rRNA transcription, AGS and 44As3 cells transfected with siCont or siDDX27 for 48 h were subjected to qRT-PCR for the 47S and 45S pre-rRNA transcripts (n=3). The expression level of siCont-transfected cells was set at 1. NS; not significant. C. To determine the rate of global protein synthesis, AGS and 44As3 cells transfected with siCont or siDDX27 for 72 h were subjected to [^{35}S]methionine incorporation assay. Equal loading of the proteins are shown by staining with Coomassie brilliant blue (CBB). Intensities of protein bands labeled with [^{35}S]methionine were not reduced after transfection with siDDX27, suggesting that the rate of global protein synthesis may not be affected by DDX27 depletion. D. AGS and 44As3 cells transfected with siCont or siDDX27 for 72 h or 96 h were subjected to Western blot analysis using antibodies against DDX27, TP53, CDKN1A and tubulin, the latter being used as an internal control. NS; not significant.

cells showed a decreased proportion in S phase and an increased proportion in G2/M phase; aneuploid (>4N) cells were also observed (**Figure 6C**, right). Because the decrease in S-phase cells was common to both cell lines, we determined the rate of DNA synthesis after transfection with siRNAs. As shown in **Figure 6D**, the rate of DNA synthesis was suppressed to a greater degree than the rate of cell proliferation (the reduction in proliferation versus the DNA synthesis rate was 9.1% versus 36.7% and 29.1% versus 56% for AGS and 44As3, respectively). Furthermore, we found that the proportion of cells positive for pHH3, a marker of mitosis, was also commonly decreased in both AGS and 44As3 cells after knockdown of DDX27 (**Figure 6E**). These results suggest that, in GC cells, DDX27 may contribute to cell growth by regulating cell cycle progression independently of apoptosis.

Knockdown of DDX27 does not affect the rates of pre-rRNA and global protein synthesis in GC cells

To address the biological function of DDX27, we analyzed the subcellular localization of DDX27 in GC cells by immunocytochemistry. As shown in **Figure 7A**, DDX27 was localized in the nucleolus, consistent with the result of immunohistochemistry (**Figure 2A**). In the nucleolus, rRNA is transcribed, processed and assembled with ribosomal proteins into large and small ribosomal subunits [46]. Therefore, we first tested the possibility that DDX27 might be involved in some of these processes and regulate global protein synthesis. However, DDX27 knockdown affected neither the rate of pre-rRNA transcription as determined by qRT-PCR of 45S and 47S pre-rRNAs (**Figure 7B**), nor that of global protein synthesis in AGS and 44As3 cells (**Figure 7C**), suggesting that DDX27 may not function in the regulation of ribosomal biogenesis in GC cells. Aside from its role in ribosomal biogenesis, it has been reported that the nucleolus regulates TP53 accumulation in response to various stressors, such as DNA damage, ribosomal stress and oncogenic stress [47]. Therefore, we next tested the possibility that DDX27 may regulate the expression of TP53 through a stress response mechanism in the nucleolus. Sequencing analysis revealed that AGS and 44As3 cells had wild-type and deleted TP53, respectively (data not shown). As shown in **Figure 7D**, while 44As3 never showed TP53 expression even after transfection with siDDX27, AGS showed substantial induction of TP53 with increased expression of CDKN1A, a molecule lying downstream of TP53, upon DDX27 knockdown, suggesting that G1 arrest in AGS cells (**Figure 6C**) may be attributable to accumulation of TP53 after transfection with siDDX27. Thus, our data suggest that DDX27 may be involved in cell cycle control in GC cells through both TP53-dependent and independent mechanisms.

Discussion

In this study, we showed that DDX27 is frequently overexpressed in GC tissues and that its expression is an independent prognostic marker for patients with GC. Furthermore, knockdown of DDX27 reduced the ability of GC cells to form colonies in soft agar. Based on these results, we propose that DDX27 could be a novel target gene for GC with 20q13 gain. During the preparation of this manuscript, Zhou et al. performed an integrated analysis of mRNA, DNA copy number and methylation status in GC tissues, and identified DDX27 as one of 126 multi-regulated genes [34]. Both we and they demonstrated upregulation of DDX27 in a substantial proportion of GCs using immunohistochemistry, confirming the upregulation of DDX27 in two independent data sets. In terms

of the function of DDX27, we focused on its involvement in the metastatic phenotype of GC cells and showed that it contributed to cell colony formation, whereas Zhou et al. focused on its role in the drug sensitivity of GC cells and concluded that depletion of DDX27 sensitizes GC cells to epirubicin and cisplatin [34]. Despite the difference in conclusions between the studies, the data from both groups suggest that expression of DDX27 might regulate important aspects of gastric carcinogenesis, such as metastasis and drug sensitivity, and serve as a useful diagnostic and therapeutic target.

In this study, we found that high expression of DDX27 in GC was associated with liver metastasis. To undergo the whole process of metastasis, which consists of multiple steps including intravasation, translocation from the primary site to a distant organ, extravasation and adaptation to the metastatic site, cancer cells must acquire the abilities to invade, survive and proliferate from a single cell or a small cluster of cells [42]. We found that knockdown of DDX27 reduced the ability of GC cells to form colonies, but had little effect on their invasiveness, suggesting that DDX27 is involved in the colony-forming ability of GC cells rather than their invasiveness. To date, although the mechanisms underlying the invasion of cancer cells into the surrounding stroma and their intravasation into the circulatory system have been relatively well established, the mechanisms involved in the subsequent steps, such as survival in the circulation and colonization of the metastatic site, remain largely unknown, because most of the genes identified as being metastasis-related reportedly contribute to cancer cell invasiveness [48]. Therefore, clarifying the mechanism of how DDX27 regulates colony formation might provide a much better understanding of the process of GC cell metastasis.

DDX27 expression was also associated with venous invasion by GC cells. We judged venous invasion according to the Japanese Classification of Gastric Carcinoma [35], in which cancer cells within veins of the gastric wall were considered to be venous positive. Generally, cancer cells within the veins of the gastric wall have been detected not as single cells but as cell clusters [35]. Although it has not yet been determined whether these clusters originate from a single intravasated cell in a manner similar to that described previously [49] or from cells that have collectively invaded from primary sites [50], our data suggest that DDX27 may contribute to the intravascular proliferation of cancer cells to form cell clusters.

In this study, we found that suppression of colony formation occurred through inhibition of the cell cycle, independently of apoptosis. It has been reported that Drs1p, the *Saccharomyces cervisiae* homologue of DDX27, localizes to the nucleolus and is required for maturation of the 60S ribosomal subunit [51]. In fact, we also observed that, in GC cells, DDX27 localizes to the nucleolus, a nuclear compartment known to play a role in ribosomal biogenesis [46]. Therefore, we initially hypothesized that inhibition of GC cell growth by DDX27 depletion might be caused by suppression of protein synthesis due to perturbation of ribosomal biogenesis. However, DDX27 depletion had little effect on protein synthesis in GC cells, suggesting that cell cycle inhibition by DDX27 depletion was not due to defects in protein synthesis. In a TP53 wild-type AGS cell line, knockdown of DDX27 induced G1 arrest accompanied by accumulation of TP53. It has been well documented that various types of nucleolus stressors, such as DNA damage, ribosomal stress and oncogenic stress, induce accumulation of TP53 and apoptosis or G1 cell cycle arrest [47]. Initially, it would seem unlikely that DNA damage would be a major cause of TP53 accumulation because phospho-histone H2AX, a marker of DNA damage, was not observed for at least 96 h after DDX27 knockdown (data not shown). Furthermore, ribosomal stress, which is reportedly caused by disruption of ribosomal biogenesis [52], would also seem unlikely, because knockdown of DDX27 in AGS had little effect on either the rate of rRNA transcription or global protein synthesis, indicating that ribosome biogenesis remains intact after DDX27 knockdown. Taken together, our data indicate that DDX27 may induce TP53-dependent cell cycle arrest in AGS cells through mechanisms other than a DNA damage response or ribosomal stress. On the other hand, in TP53-deleted 44As3 cells, DDX27 depletion did not induce G1 arrest, but caused G2 arrest accompanied by an increase of aneuploid cells, leading to inhibition of cell cycle progression. Although the mechanisms underlying these cell cycle defects are largely unknown, DNA damage and ribosomal stress may not play a role, because knockdown of DDX27 induced neither accumulation of phospho-histone H2AX nor suppression of global protein synthesis before the cell

cycle defects appeared (<96 h) in this cell line. To date, nucleolar proteins that have been reported to function in cell cycle control mainly exert their function through regulation of TP53 stabilization [33, 53]. Because a large proportion of solid tumors harbor mutation in TP53, clarification of the mechanism whereby DDX27 regulates the cell cycle independently of TP53 might yield a new strategy for finding a novel targetable pathway in GC.

Based on our present data, we speculate that targeting DDX27 or its related molecules might be effective in GC patients, because DDX27 is upregulated in a large proportion of GCs and knockdown of DDX27 inhibited colony formation by both TP53 wild-type and deleted cells, suggesting that selection of patients on the basis of TP53 status might not be necessary. Further studies will be required to explore the potential of DDX27 as a therapeutic target in GC patients.

Acknowledgements

We would like to thank Ms. Misuzu Taguchi for her excellent experimental assistance. We would like to dedicate this manuscript to Dr. Tsuyoshi Noguchi, one of the study co-authors, who passed away before publication. This work was supported in part by JSPS KAKENHI Grant Number 24590446.

Disclosure of conflict of interest

None.

Address correspondence to: Yoshiyuki Tsukamoto, Department of Molecular Pathology, Faculty of Medicine, Oita University, Hasama-machi, Yufu-City, Oita 879-5593, Japan. Fax: 81-97-586-5699; E-mail: tuka@oita-u.ac.jp

References

[1] Tsukamoto Y, Uchida T, Karnan S, Noguchi T, Nguyen LT, Tanigawa M, Takeuchi I, Matsuura K, Hijiya N, Nakada C, Kishida T, Kawahara K, Ito H, Murakami K, Fujioka T, Seto M and Moriyama M. Genome-wide analysis of DNA copy number alterations and gene expression in gastric cancer. J Pathol 2008; 216: 471-482.

[2] Carvalho B, Buffart TE, Reis RM, Mons T, Moutinho C, Silva P, van Grieken NC, Grabsch H, van de Velde CJ, Ylstra B, Meijer GA and Carneiro F. Mixed gastric carcinomas show similar chromosomal aberrations in both their diffuse and glandular components. Cell Oncol 2006; 28: 283-294.

[3] Kimura Y, Noguchi T, Kawahara K, Kashima K, Daa T and Yokoyama S. Genetic alterations in 102 primary gastric cancers by comparative genomic hybridization: gain of 20q and loss of 18q are associated with tumor progression. Mod Pathol 2004; 17: 1328-1337.

[4] Kokkola A, Monni O, Puolakkainen P, Nordling S, Haapiainen R, Kivilaakso E and Knuutila S. Presence of high-level DNA copy number gains in gastric carcinoma and severely dysplastic adenomas but not in moderately dysplastic adenomas. Cancer Genet Cytogenet 1998; 107: 32-36.

[5] Noguchi T, Wirtz HC, Michaelis S, Gabbert HE and Mueller W. Chromosomal imbalances in gastric cancer. Correlation with histologic subtypes and tumor progression. Am J Clin Pathol 2001; 115: 828-834.

[6] Takada H, Imoto I, Tsuda H, Sonoda I, Ichikura T, Mochizuki H, Okanoue T and Inazawa J. Screening of DNA copy-number aberrations in gastric cancer cell lines by array-based comparative genomic hybridization. Cancer Sci 2005; 96: 100-110.

[7] Fan B, Dachrut S, Coral H, Yuen ST, Chu KM, Law S, Zhang L, Ji J, Leung SY and Chen X. Integration of DNA copy number alterations and transcriptional expression analysis in human gastric cancer. PLoS One 2012; 7: e29824.

[8] Hidaka S, Yasutake T, Kondo M, Takeshita H, Yano H, Haseba M, Tsuji T, Sawai T, Nakagoe T and Tagawa Y. Frequent gains of 20q and losses of 18q are associated with lymph node metastasis in intestinal-type gastric cancer. Anticancer Res 2003; 23: 3353-3357.

[9] Scotto L, Narayan G, Nandula SV, Arias-Pulido H, Subramaniyam S, Schneider A, Kaufmann AM, Wright JD, Pothuri B, Mansukhani M and Murty VV. Identification of copy number gain and overexpressed genes on chromosome arm 20q by an integrative genomic approach in cervical cancer: potential role in progression. Genes Chromosomes Cancer 2008; 47: 755-765.

[10] Sonoda G, Palazzo J, du Manoir S, Godwin AK, Feder M, Yakushiji M and Testa JR. Comparative genomic hybridization detects frequent overrepresentation of chromosomal material from 3q26, 8q24, and 20q13 in human ovarian carcinomas. Genes Chromosomes Cancer 1997; 20: 320-328.

[11] Tsafrir D, Bacolod M, Selvanayagam Z, Tsafrir I, Shia J, Zeng Z, Liu H, Krier C, Stengel RF, Barany F, Gerald WL, Paty PB, Domany E and Notterman DA. Relationship of gene expression and chromosomal abnormalities in colorectal cancer. Cancer Res 2006; 66: 2129-2137.

[12] Hodgson JG, Chin K, Collins C and Gray JW. Genome amplification of chromosome 20 in breast cancer. Breast Cancer Res Treat 2003; 78: 337-345.
[13] Alers JC, Krijtenburg PJ, Vis AN, Hoedemaeker RF, Wildhagen MF, Hop WC, van Der Kwast TT, Schroder FH, Tanke HJ and van Dekken H. Molecular cytogenetic analysis of prostatic adenocarcinomas from screening studies: early cancers may contain aggressive genetic features. Am J Pathol 2001; 158: 399-406.
[14] Mahlamaki EH, Barlund M, Tanner M, Gorunova L, Hoglund M, Karhu R and Kallioniemi A. Frequent amplification of 8q24, 11q, 17q, and 20q-specific genes in pancreatic cancer. Genes Chromosomes Cancer 2002; 35: 353-358.
[15] Nancarrow DJ, Handoko HY, Smithers BM, Gotley DC, Drew PA, Watson DI, Clouston AD, Hayward NK and Whiteman DC. Genome-wide copy number analysis in esophageal adenocarcinoma using high-density single-nucleotide polymorphism arrays. Cancer Res 2008; 68: 4163-4172.
[16] Hurst CD, Fiegler H, Carr P, Williams S, Carter NP and Knowles MA. High-resolution analysis of genomic copy number alterations in bladder cancer by microarray-based comparative genomic hybridization. Oncogene 2004; 23: 2250-2263.
[17] Tabach Y, Kogan-Sakin I, Buganim Y, Solomon H, Goldfinger N, Hovland R, Ke XS, Oyan AM, Kalland KH, Rotter V and Domany E. Amplification of the 20q chromosomal arm occurs early in tumorigenic transformation and may initiate cancer. PLoS One 2011; 6: e14632.
[18] van Dekken H, Paris PL, Albertson DG, Alers JC, Andaya A, Kowbel D, van der Kwast TH, Pinkel D, Schroder FH, Vissers KJ, Wildhagen MF and Collins C. Evaluation of genetic patterns in different tumor areas of intermediate-grade prostatic adenocarcinomas by high-resolution genomic array analysis. Genes Chromosomes Cancer 2004; 39: 249-256.
[19] Postma C, Terwischa S, Hermsen MA, van der Sijp JR and Meijer GA. Gain of chromosome 20q is an indicator of poor prognosis in colorectal cancer. Cell Oncol 2007; 29: 73-75.
[20] Hirasaki S, Noguchi T, Mimori K, Onuki J, Morita K, Inoue H, Sugihara K, Mori M and Hirano T. BAC clones related to prognosis in patients with esophageal squamous carcinoma: an array comparative genomic hybridization study. Oncologist 2007; 12: 406-417.
[21] Shridhar V, Lee J, Pandita A, Iturria S, Avula R, Staub J, Morrissey M, Calhoun E, Sen A, Kalli K, Keeney G, Roche P, Cliby W, Lu K, Schmandt R, Mills GB, Bast RC Jr, James CD, Couch FJ, Hartmann LC, Lillie J and Smith DI. Genetic analysis of early-versus late-stage ovarian tumors. Cancer Res 2001; 61: 5895-5904.
[22] Carvalho B, Postma C, Mongera S, Hopmans E, Diskin S, van de Wiel MA, van Criekinge W, Thas O, Matthai A, Cuesta MA, Terhaar Sive Droste JS, Craanen M, Schrock E, Ylstra B and Meijer GA. Multiple putative oncogenes at the chromosome 20q amplicon contribute to colorectal adenoma to carcinoma progression. Gut 2009; 58: 79-89.
[23] Uchida M, Tsukamoto Y, Uchida T, Ishikawa Y, Nagai T, Hijiya N, Nguyen LT, Nakada C, Kuroda A, Okimoto T, Kodama M, Murakami K, Noguchi T, Matsuura K, Tanigawa M, Seto M, Ito H, Fujioka T, Takeuchi I and Moriyama M. Genomic profiling of gastric carcinoma in situ and adenomas by array-based comparative genomic hybridization. J Pathol 2010; 221: 96-105.
[24] Bruin SC, Klijn C, Liefers GJ, Braaf LM, Joosse SA, van Beers EH, Verwaal VJ, Morreau H, Wessels LF, van Velthuysen ML, Tollenaar RA and Van't Veer LJ. Specific genomic aberrations in primary colorectal cancer are associated with liver metastases. BMC Cancer 2010; 10: 662.
[25] Hidaka S, Yasutake T, Takeshita H, Kondo M, Tsuji T, Nanashima A, Sawai T, Yamaguchi H, Nakagoe T, Ayabe H and Tagawa Y. Differences in 20q13.2 copy number between colorectal cancers with and without liver metastasis. Clin Cancer Res 2000; 6: 2712-2717.
[26] Fujita Y, Sakakura C, Shimomura K, Nakanishi M, Yasuoka R, Aragane H, Hagiwara A, Abe T, Inazawa J and Yamagishi H. Chromosome arm 20q gains and other genomic alterations in esophageal squamous cell carcinoma, as analyzed by comparative genomic hybridization and fluorescence in situ hybridization. Hepatogastroenterology 2003; 50: 1857-1863.
[27] Sillars-Hardebol AH, Carvalho B, Tijssen M, Belien JA, de Wit M, Delis-van Diemen PM, Ponten F, van de Wiel MA, Fijneman RJ and Meijer GA. TPX2 and AURKA promote 20q amplicon-driven colorectal adenoma to carcinoma progression. Gut 2012; 61: 1568-1575.
[28] Littlepage LE, Adler AS, Kouros-Mehr H, Huang G, Chou J, Krig SR, Griffith OL, Korkola JE, Qu K, Lawson DA, Xue Q, Sternlicht MD, Dijkgraaf GJ, Yaswen P, Rugo HS, Sweeney CA, Collins CC, Gray JW, Chang HY and Werb Z. The transcription factor ZNF217 is a prognostic biomarker and therapeutic target during breast cancer progression. Cancer Discov 2012; 2: 638-651.
[29] Jang SH, Park JW, Kim HR, Seong JK and Kim HK. ADRM1 gene amplification is a candidate driver for metastatic gastric cancers. Clin Exp Metastasis 2014; 31: 727-733.
[30] Jarmoskaite I and Russell R. DEAD-box proteins as RNA helicases and chaperones. Wiley Interdiscip Rev RNA 2011; 2: 135-152.

[31] Parsyan A, Shahbazian D, Martineau Y, Petroulakis E, Alain T, Larsson O, Mathonnet G, Tettweiler G, Hellen CU, Pestova TV, Svitkin YV and Sonenberg N. The helicase protein DHX29 promotes translation initiation, cell proliferation, and tumorigenesis. Proc Natl Acad Sci U S A 2009; 106: 22217-22222.

[32] Mazurek A, Luo W, Krasnitz A, Hicks J, Powers RS and Stillman B. DDX5 regulates DNA replication and is required for cell proliferation in a subset of breast cancer cells. Cancer Discov 2012; 2: 812-825.

[33] Fukawa T, Ono M, Matsuo T, Uehara H, Miki T, Nakamura Y, Kanayama HO and Katagiri T. DDX31 regulates the p53-HDM2 pathway and rRNA gene transcription through its interaction with NPM1 in renal cell carcinomas. Cancer Res 2012; 72: 5867-5877.

[34] Zhou J, Yong WP, Yap CS, Vijayaraghavan A, Sinha RA, Singh BK, Xiu S, Manesh S, Ngo A, Lim A, Ang C, Xie C, Wong FY, Lin SJ, Wan WK, Tan I, Flotow H, Tan P, Lim KH, Yen PM and Goh LK. An Integrative Approach Identified Genes Associated with Drug Response in Gastric Cancer. Carcinogenesis 2015; 36: 441-51.

[35] Japanese Gastric Cancer Association. Japanese Classification of Gastric Carcinoma-2nd English Edition. Gastric Cancer 1998; 1: 10-24.

[36] Lauren P. The Two Histological Main Types of Gastric Carcinoma: Diffuse and So-Called Intestinal-Type Carcinoma. An Attempt at a Histo-Clinical Classification. Acta Pathol Microbiol Scand 1965; 64: 31-49.

[37] Yanagihara K, Ito A, Toge T and Numoto M. Antiproliferative effects of isoflavones on human cancer cell lines established from the gastrointestinal tract. Cancer Res 1993; 53: 5815-5821.

[38] Yanagihara K, Takigahira M, Tanaka H, Komatsu T, Fukumoto H, Koizumi F, Nishio K, Ochiya T, Ino Y and Hirohashi S. Development and biological analysis of peritoneal metastasis mouse models for human scirrhous stomach cancer. Cancer Sci 2005; 96: 323-332.

[39] Moriyama M, Tsukamoto Y, Fujiwara M, Kondo G, Nakada C, Baba T, Ishiguro N, Miyazaki A, Nakamura K, Hori N, Sato K, Shomori K, Takeuchi K, Satoh H, Mori S and Ito H. Identification of a novel human ankyrin-repeated protein homologous to CARP. Biochem Biophys Res Commun 2001; 285: 715-723.

[40] Matsuo M, Nakada C, Tsukamoto Y, Noguchi T, Uchida T, Hijiya N, Matsuura K and Moriyama M. MiR-29c is downregulated in gastric carcinomas and regulates cell proliferation by targeting RCC2. Mol Cancer 2013; 12: 15.

[41] Cui C and Tseng H. Estimation of ribosomal RNA transcription rate in situ. Biotechniques 2004; 36: 134-138.

[42] Valastyan S and Weinberg RA. Tumor metastasis: molecular insights and evolving paradigms. Cell 2011; 147: 275-292.

[43] Hicks GG, Egan SE, Greenberg AH and Mowat M. Mutant p53 tumor suppressor alleles release ras-induced cell cycle growth arrest. Mol Cell Biol 1991; 11: 1344-1352.

[44] Wagner AJ, Small MB and Hay N. Myc-mediated apoptosis is blocked by ectopic expression of Bcl-2. Mol Cell Biol 1993; 13: 2432-2440.

[45] Zhu Q, Yasumoto H and Tsai RY. Nucleostemin delays cellular senescence and negatively regulates TRF1 protein stability. Mol Cell Biol 2006; 26: 9279-9290.

[46] Hernandez-Verdun D. The nucleolus: a model for the organization of nuclear functions. Histochem Cell Biol 2006; 126: 135-148.

[47] Boulon S, Westman BJ, Hutten S, Boisvert FM and Lamond AI. The nucleolus under stress. Mol Cell 2010; 40: 216-227.

[48] Chaffer CL and Weinberg RA. A perspective on cancer cell metastasis. Science 2011; 331: 1559-1564.

[49] Al-Mehdi AB, Tozawa K, Fisher AB, Shientag L, Lee A and Muschel RJ. Intravascular origin of metastasis from the proliferation of endothelium-attached tumor cells: a new model for metastasis. Nat Med 2000; 6: 100-102.

[50] Cheung KJ and Ewald AJ. Illuminating breast cancer invasion: diverse roles for cell-cell interactions. Curr Opin Cell Biol 2014; 30: 99-111.

[51] Ripmaster TL, Vaughn GP and Woolford JL Jr. A putative ATP-dependent RNA helicase involved in Saccharomyces cerevisiae ribosome assembly. Proc Natl Acad Sci U S A 1992; 89: 11131-11135.

[52] Zhang Y and Lu H. Signaling to p53: ribosomal proteins find their way. Cancer Cell 2009; 16: 369-377.

[53] Sasaki M, Kawahara K, Nishio M, Mimori K, Kogo R, Hamada K, Itoh B, Wang J, Komatsu Y, Yang YR, Hikasa H, Horie Y, Yamashita T, Kamijo T, Zhang Y, Zhu Y, Prives C, Nakano T, Mak TW, Sasaki T, Maehama T, Mori M and Suzuki A. Regulation of the MDM2-P53 pathway and tumor growth by PICT1 via nucleolar RPL11. Nat Med 2011; 17: 944-951.